TR－A－0046

A Compuational Cochlear Nonlinear Preprocessing Model with Adaptive Q Circuits

平原　達也

Tatsuya Hirahara

1989. 2. 13

ＡＴＲ視聴覚機構研究所

A Computational Cochlear Nonlinear Preprocessing Model with Adaptive Q Circuits

Tatsuya Hirahara

ATR Auditory and Visual Perception Research Laboratories
Twin 21 MID Tower, 2-1-61 Shiromi, Higashi-ku, Osaka 540, Japan

Abstract

A computational nonlinear cochlear filter model with adaptive Q circuits is described. The model is build by introducing adaptive Q circuits into the linear cascade/parallel cochlear filter-bank. The adaptive Q circuit is composed of two part: a second order low-pass function (LPF) and a Q decision circuit which calculates LPF's Q in every time frame according to the input spectrum level. This model functionally simulates three level dependent characteristics observed in the basilar membrane motion: level dependent selectivity, level dependent sensitivity and level dependent resonance frequency shift. The model output gives better internal speech spectrum representation than those of a linear cochlear filter-bank. Namely, (1) weak consonants and higher formants are enhanced, (2) both the temporal and the harmonic structure are consistent at the same time frame, and (3) the spectrum are spread and enhanced where the spectrum changes abruptly. These advantages, which are the phenomena observed in the real auditory frequency analysis, support the effectiveness of the model.

Introduction

The spectral analysis performed in the auditory pathway is quite different from spectral analysis based upon the digital signal processing we usually use. This means that the internal spectrum, the sound spectrum representation in the auditory pathway, differs from the physical spectrum. Hence we believe the internal spectrum is superior to the physical spectrum when discussing perceptual cues of speech, evaluating the quality of synthesized speech or using it as an input vector of an automatic speech recognition system.

In order to obtain the internal spectrum representation, there have been many attempts to build an auditory model which adequately reflects the sound spectral transformation that takes place in the human auditory pathway, particularly in the cochlea . The cochlea is a nonlinear spectral analyzer composed of two systems: the basilar membrane vibrating system which performs an active nonlinear filtering with outer hair cells, and the inner

hair cell system which activates the eighth-nerve according to the basilar membrane displacement.

Many previous auditory models tried to simulate this nonlinear signal processing in the cochlea using a linear filter bank stage followed by a nonlinear processing stage. In those auditory models, several basic auditory functions, such as level dependent filtering characteristics, could not be realized since nonlinear basilar membrane motion was simulated by a linear filter.[Lyon(1982), Allen(1985), Shamma(1985), Seneff(1986), Ghitza (1986), Linngard (1986), Komakine *et al.* (1988)]

On the other hand, there are several nonlinear basilar membrane models which deal with active vibrating mechanisms of the basilar membrane.[de Bore(1983), Neely *et al.*(1985), Kohda(1986), Li Deng *et al.* (1987)] Although many of these models are described by partial differential equations based on cochlear hydrodynamics, they require considerable computational time to produce the model output. A few models succeeded in building an efficient nonlinear cochlear preprocessing model by using an analogue circuit [Zwicker (1986), Lyon *et al.* (1988)].

In this paper, we describe an efficient computational model of the nonlinear filtering performed at the basilar membrane system that is constructed by introducing adaptive Q circuits to the cascade/parallel linear cochlear filter-bank. We show the details of the nonlinear cochlear filter with adaptive Q circuits and discuss the model characteristics. Then the spectrogram obtained by the proposed model is compared with that of the traditional linear cochlear filter-bank.

Nonlinearity of the basilar membrane system

Since von Békésy observed basilar membrane motion, it had been believed that the basilar membrane is a passive linear system having a broad frequency selectivity. However, observations of the basilar membrane motion in fully functioning cochlear indicated that the basilar membrane itself has very sharp frequency selectivity for low sound pressure level input as measured neuro-physiologically at the eighth-nerve.[Khanna *et*

al.(1982), Sellick *et al.* (1982)] Moreover, it is shown that the transfer characteristics of the basilar membrane system vary depending on the input signal level. Furthermore, findings of the cochlear echo [Kemp (1980)] and studies on oto-acoustic emission [Zurek (1980)] suggest that the basilar membrane is an active system.

In Fig.1, basilar membrane displacement observed at the place corresponding to 18kHz for four sound pressure levels is plotted as a function of input signal frequency. [replotted from B.Johnstone *et al.*, (1986)]. In Fig.1, three interesting points of behavior of the basilar membrane motion are indicated; (1) level-dependent frequency selectivity, (2) level-dependent nonlinear reduction of the relative gain at the resonance frequency, and (3) level-dependent resonance frequency shift. The first two characteristics make the basilar membrane system an excellent spectral analyzer, that is, increasing the signal-to-noise ratio for weak components of the input by increasing not only the gain but also the resonance Q of the channel. However, the advantage of the third point of behavior for an auditory spectral analyzer is not yet known.

An adaptive Q circuit

In order to simulate nonlinearity of the basilar membrane system mentioned above, the adaptive Q circuit in Fig.2 is introduced. The adaptive Q circuit consists of two parts; a second order low-pass function and a Q decision circuit.

First, when the gain at DC is set at unity, the transfer function of the second order low-pass function LPF(s) is given by

$$LPF(s) = \frac{\omega_1^2}{s^2 + (\omega_1/Q_1)s + \omega_1^2} \qquad [1]$$

where ω_1 and Q_1 are the pole frequency in radian and the Q (quality factor) at the pole, respectively. Its magnitude frequency response

$$|LPF(j\omega)| = \frac{Q_1}{\sqrt{Q_1^2\{1-(\omega/\omega_1)^2\}^2+(\omega/\omega_1)^2}} \qquad [2]$$

is shown in Fig.2 for four Q_l values. The maximum value of $|LPF(j\omega)|$ is

$$G_{max} = |LPF(j\omega_{max})| = \frac{Q_l}{\sqrt{1-1/(4Q_l^2)}} \quad [3]$$

where

$$\omega_{max} = \{1-1/(2Q_l^2)\}\omega_l \quad [4]$$

When Q_l is large, the formulae [3] and [4] show that the second order low-pass function reaches a maximum gain Q_l at $\omega=\omega_l$. At this time, its transfer characteristic is that of a low-pass filter with a single resonance at ω_l and with Q of the resonance nearly equal to Q_l. Then, the decrease in Q_l brings the reduction of G_{max}, the lower shift of ω_{max} and the Q decrease simultaneously. When Q_l is below $1/\sqrt{2}$, the transfer characteristic becomes that of a simple low-pass filter, where ω_l and Q_l are not significant. This means that we can control the maximum gain, the resonance frequency and the Q, simultaneously by choosing adequate values of Q_l.

Next, let us consider a Q-decision circuit which calculates $Q_l(t)$, the Q of the second order low-pass function at the time frame t, from controlling signal y(t) in every time frame using the following formulae.

$$Q_l(t) = \begin{cases} Qmax & \rho(t) \le \rho min \\ Qmax\{1-\dot{\rho}(t)^{\alpha}\}+Qmin & \rho min \le \rho(t) \le \rho max \\ Qmin & \rho max \le \rho(t) \end{cases} \quad [5]$$

where

$$\dot{\rho}(t) = (\rho(t) - \rho min)/(\rho rmax - \rho min) \quad [6]$$

While Qmax, Qmin, ρmax, ρmin and a are constant, $\rho(t)$ is the logarithmic power of the controlling signal at time frame t, which is given by

$$\rho(t) = \log\left(\int_{t=t-\delta}^{t} |y(t)|dt/\delta\right) \quad [7]$$

where δ is a constant which determines the renewal period of $Q_l(t)$. The input-output function of the Q-decision circuit for $\alpha=1$ is shown in Fig.2. This Q-decision circuit generates the largest Q_l when $\rho(t)$ is smaller than rmin and the smallest Q_l when $\rho(t)$ is greater than rmax. When $\rho(t)$ is between ρmin and ρmax, an intermediate Q_l value is generated inversely proportional to $\rho(t)$.

Cochlear filter with adaptive Q circuits

There are several ways to build a cochlear filter-bank with the adaptive Q circuit. Fig.3(a) shows a parallel type system in which adaptive Q circuits are connected to each output of the N channel parallel band-pass filter bank. Fig.3(b) shows a cascade type system where the N adaptive Q circuits are connected in cascade. R.F.Lyon's analogue cochlear LSI has this architecture. Fig.3(c) shows a cascade/ parallel type system in which adaptive Q circuits are connected to each output of the N channel cascade/parallel filter bank, as shown in Fig.3.

We chose the cascade/parallel type architecture to build a model since cascade/parallel type filter well simulate not only the amplitude but also the phase characteristics of the real cochlea with less difficulty than the other types. In Fig.4, the i-the section's block diagram of the cascade/parallel nonlinear cochlear filter model with adaptive Q circuits is shown. In the model, first, the i cascaded low-pass type notch filters form a low-pass filter with very sharp cut off characteristics. Next, by connecting a band-pass filter BPF_i to the i-th notch filter's output, the transfer characteristics from system input to BPF_i output become those of an asymmetrical band-pass filter with steep high cut off and gradual tail at lower frequency. Finally, the output of the BPF_i is led to the second order low-pass function LPF_i of the i-th adaptive Q circuit, where the output of the BPF_i is also fed forward as the control signal of the Q-decision circuit.

Transfer functions and parameters of each part of the model are summarized in Table 1. Parameters of notch filters and band-pass filters are determined by the same procedure as in the linear cascade/parallel cochlear filter. The only difference is that Qb, the value of each band-pass filter's Q, takes a smaller value in the model (Qb=4.5) compared with in the linear model (Qb=20 to 50), since Qb determines the minimum effective Q value of each channel for the maximum input level in the model.

In the model, Rl, the ratio of ωb_i to ωl_i, is set up to be greater than 1 so as to lower the resonance frequency of each channel according to the Ql_i decrease. When $Rl_i=1$, the resonance frequency is only slightly affected by the Ql_i.

Characteristics of the model

In this section, several characteristics of the proposed model are described. The model consists of a 61 channel nonlinear cascade/parallel type cochlear filter with adaptive Q circuits spanning the frequency region from 1 to 21 Bark in 1/3 Bark increment. In the model, the frequency scale transformation from Hz to Bark is performed by Zwicker's formula (Zwicker *et al.* 1980). Furthermore, the relation between the channel number i and the Bark frequency is i=3*Bark.

Amplitude frequency responses for the 27th channel of the model for five input levels (Lin) are depicted in Fig.5. This plot shows the frequency response for a certain place. As shown in Fig.5, the model realizes asymmetrical band-pass characteristics with three level dependent characteristics: resonance Q decreases as Lin increases, relative gain at resonance decreases as Lin increases and the resonance frequency shifts lower as Lin increases.

Fig.6 shows the place response for a certain frequency for a 9 Bark pure tone at five input levels. Such a plot shows the equivalent of the basilar membrane displacement along the basilar membrane on a logarithmic scale. As shown in Fig.6, for high input levels, the place response shows broad peak, whereas for low input levels, the response sharply peaks indicating that the adaptive Q circuits produce sharp tuning at low input levels. In addition, it shows that the model reflects the basilar membrane vibration, in which displacement is large at the place down to the place of the input signal frequency while it is suddenly dumped beyond that place.

Fig.7 shows effective Q of several channels as a function of Ql. Since amplitude frequency response of each channel is asymmetrical against the resonance frequency, the effective Q of each channel is defined by

$$Qeff = (\omega^+ - \omega^-)/\omega_0 \qquad [8]$$

where ω^+ and ω^- represent upper and lower -3dB frequency and ω_0 is the resonance frequency. Effective Q of each channel is determined by the sharp role off characteristics of cascaded notch filters, Qb and Ql, thus the Qeff varies in proportion to the Ql.

Fig.8 shows the maximum gain of several channel as a function of Ql. The maximum gain of each channel is determined by the second order low-pass filter's gain in the adaptive Q circuit, then increases in logarithmically as Ql increases. Since the gain of the filters before adaptive Q circuits are not flat, the maximum gains of the 60th channel (20 Bark) is smaller than the others.

Spectral analysis by the model

Sound spectrograms obtained by three types of cochlear filter models are shown in Fig.9 Fig.9(a) and (b) show the spectrogram obtained by a cascade/parallel linear cochlear filter-bank without adaptive Q circuits, in which Qs are fixed: (a) Qb=4.5 and (b) Qb=30. Fig.9(c) shows that obtained by the proposed nonlinear cochlear filter-bank with adaptive Q circuits. Each filter has 61 channels covering 1 to 21 Bark in 1/3 bark increment (3rd to 63rd channels). In each spectrogram, the logarithmic power of each filter output calculated using a 2 msec. rectangular window without overlapping are represented in 36 gray levels with an 80dB dynamic range. Input speech is the Japanese sentence "Sangatsu kokonoka" (March ninth) spoken by a male, which is sampled at 20kHz with 16 bit accuracy.

Weak consonants, such as unvoiced fricative /s/, /tsu/ and voiceless stop /k/, and higher formants are represented more clearly in the spectrogram by the adaptive Q filter (c) than spectrograms by fixed Q filters (a) or (b). These enhancements are the result of an AGC effect brought by the variable gain characteristics of the adaptive Q circuit.

The low Q filtering provides good time resolution, black vertical stripes synchronized with the fundamental period are seen in Fig.9(a). The high Q filtering however provides good frequency resolution, horizontal stripes, which are the harmonic components of the fundamental frequency (F0), seen in Fig.9(b). On the other hand, both the time and the frequency resolution are high in *the same time frame* in Fig.9(c), since the filtering Q of each channel is varied according to the spectral level of each channel at every time frame. For example, the F0 harmonic

structure seen in the lower frequency region of the vowel part (lower than the 21st channel) is the proof of the high Q filtering, while vertical stripes seen in the higher frequency region (higher than the 21st channel) are the proof of the low Q filtering.

Fig.10 shows the spectrogram by the proposed model for a 9 Bark pure tone burst. The spectrum spreading and enhancement at onset and offset shown in Fig.10 are effects of the adaptive Q circuits. Namely, the input signal is analyzed with high Q1 at the onset since Q1 can not follow the abrupt change in the input level. This spectrum spreading and enhancement at a sudden spectral change are observed in the results of spatio-temporal masking experiments. [Miyasaka (1983), Hirahara (1987)]

Fig.11 shows spectral slices of synthesized vowel /a/ (F0=1.23, F1=6.77, F2=9.63, F3=14.73 and F4=16.94 Bark) with several input levels. Fig.11(a) shows the output of the linear cochlear filter bank with fixed Q (Qb=4.5). Fig.11(b) shows the output of the proposed nonlinear cochlear filter with adaptive Q circuit. The output spectrum of the linear filter are the same for any input level. Only the absolute spectrum level shifts according to the input level. On the other hand, the output spectrum of the nonlinear filter varies according to the input level. Spectral envelope peaks corresponding to formants are enhanced. In particular, spectral peaks corresponding to F3 and F4 become clearer by decreasing the input level.

Conclusion

In this paper, a computational cochlear nonlinear preprocessing model realized by introducing adaptive Q circuits into the cascade/parallel cochlear filter is described. This model functionally simulates three level dependent characteristics observed in the basilar membrane displacement: level dependent resonance Q change, level dependent gain reduction and level dependent resonance frequency shift.

Spectrograms obtained by the nonlinear cochlear filter with adaptive Q circuits are compared with those of an ordinary linear cascade/parallel linear cochlear filter. The advantages of the

proposed model are as follows. (1) Weak consonants and higher formants are enhanced by the AGC effect. (2) As the analysis is done by different Q value at each channel, both the temporal and the harmonic structure are consistent at the same time frame. (3) Spectra are spread and enhanced where the spectral level changes abruptly. These advantages, which are the phenomena observed in the real auditory frequency analysis, support the effectiveness of the model.

It was confirmed that speech features were represented more adequately on our auditory spectrogram than the traditional spectrogram. Therefore, we believe that well designed auditory models should be more useful in many fields of speech science, particularly in the automatic speech recognition works. However, in order to judge whether an auditory-based spectral analyzer will pay off in automatic speech recognition or not, systematic application researches, such as recognition experiments inquiring distance measures and recognition methods, are needed.

References

[1] Allen J. B.(1985), "Cochlear Modeling", IEEE ASSP Magazine, pp.3-29

[2] de Bore E. (1983) "On active and passive cochlear models-Towards a generalized analysis", J.A.S.A.,73, pp.574-576

[3] Ghitza O.(1986) "Auditory nerve representation as a front-end for speech recognition in a noisy environment", Computer Speech and Language, Vol.1, pp.109-130

[4] Johnstone B.M. *et al.* (1986),"Basilar membrane measurements and the travelling wave", Hearing Research,22, pp.147-153

[5] Kemp D.T.(1980) "Towards a model for the origin of cochlear echos", Hearing Research, vol.2, pp.533-548

[6] Kohda T.*et al.* (1986) "An exactly solvable active one-dimensional model of basilar membrane displacement without wave reflection", Acoust. Soc. Japan, Trans.H-86-60 (in Japanese)

[7] Komakine T. *et al.* (1986) "A filter-bank design for simulating cochlear frequency analysis function", IEICE Trans. SP-87-45 (in Japanese)

[8] Khanna S.M.*et al.* (1982) "Basilar membrane tuning in the cat cochlear", Science 190, pp.1218-1221

[9] Linggard R.*et.al* (1986) "A Computational Model of the Basilar Membrane", Proc. 1st Australian Conf. on Speech Science and Technology, pp.286-287

[10] Lyon R.F.(1982) "A Computational Model of Filtering, Detection and Compression in the Cochlear", Proc. ICASSP, pp.1282-1285

[11] Miyasaka E.(1983) "Spatio-temporal characteristics of masking of brief test-tone pulses by a tone-burst with abrupt switching transients", J. Acoust. Soc. Japan, vol.39, No.9, pp.614-623 (in Japanese)

[12] Neely S.T. *et al.* "An active cochlear model showing sharp tuning and high sensitivity" Hearing Research 9, pp.123-130

[13] Sellick P.M.*et al.* (1982) "Measurement of basilar membrane motion in the guinea pig using Mössbauer technique", J.A.S.A., 72, pp.131-141

[14] Seneff S.(1986) "A Computational Model for the Peripheral Auditory System: Application to Speech Recognition Research", Proc. ICASSP, pp.37.8.1-37.8.4

[15] Shamma S.A.(1985) Speech processing in the auditory system I: The representation of speech sound in the response of the auditory nerve", J.A.S.A., 78(5), pp.1622-1632

[16] Hirahara T.(1987) "Inter-aural Speech Spectrum Representation by Spatio-Temporal Masking Pattern", Proc. 11th ICPhS, vol.1, pp.92-95

[17] Hirahara T.*et al.* (1988) "Nonlinear Cochlear Filter with Adaptive Q Function", Proc. Fall meeting of IEICE, pp.A-1-109 to A-1-110 (in Japanese)

[18] von Bekesy (1960), *Experiments in Hearing* , McGraw Hill

[16] Zurek P.M.(1981) "Spontaneous narrowband acoustic signals emitted by human ears", J.A.S.A., 69, pp.514-523

[19] Zwicker E.*et al.* (1980) " Analytical expression for critical-band rate and critical bandwidth as a function of frequency", J.A.S.A.,68(5), pp.1523-1525

[20] Zwicker E. (1986) "A hardware cochlear nonlinear preprocessing model with active feedback", J.A.S.A., 80(1), pp.146-153

[21] Theme Issue, *Representation of Speech in the Auditory Periphery*, Journal of Phonetics, vol.16, No.1, pp.1-149

[22] M.R.Schroeder (1973) " An integrable model for the basilar membrane", J.Acoust.Soc.Am.,53(2), pp.429-434

[23] M.Blomberg *et al.* (1984) "Auditory models in Isolated Word Recognition", Proc. ICASSP, pp. 17.9.1-17.9.4

[24] S.A.Shamma (1986) "A biophysical model of cochlear processing: Intensity dependence of pure tone response", J.Acoust.Soc.Am., 80(1), pp.133-145

[25] M.Hunt *et al.* (1986) "Speech Recognition using a Cochlear Model", Proc. ICASSP, pp.37.7.1-37.7.4

[26] Proceedings of Montreal Symposium on Speech Recognition (1986)

[27] R.Togneri *et al.* (1986) "Fast, Stable Solution of the Two-Dimensional Cochlear Model", Proc. of the 1st Australian Conference on Speech Science and Technology, pp.292-297

[28] M.Karjalainen (1987) " Auditory Models for Speech Processing", Proc. of the 11th ICPhS Tallin, vol.2, pp.11-20

[29] Y.Sujaku (1986) " An active model of basilar membrane vibrations", Trans. Acoust.Soc.Japan H-86-61 (in Japanese)

[30] R.Guelke *et al.* (1987) "Modeling the cochlear", Electronics & Wireless World, vol.92, No.1611, pp.19-21

[31] K.Payton (1988) "Vowel processing by a model of the auditory periphery: A comparison to eighth-nerve response", J.Acoust.Soc.Am.,83(1), pp.145-162

[32] J.C.Caerou *et al.* (1987) "Modele actif du systeme auditif peripherique", Bulletin du Laboratoire de la Communication Parlee, vol.1B, pp.211-235

[33] L.Deng *et al.* (1987) "A composite auditory model for processing speech sound", J.Acoust.Soc.Am., 82(6), pp.2001-2012

[34] R.F.Lyon *et al.* (1988) " An Analogue Electronic Cochlear", IEEE Trans. ASSP, vol.36, No.7, pp.1119-1134

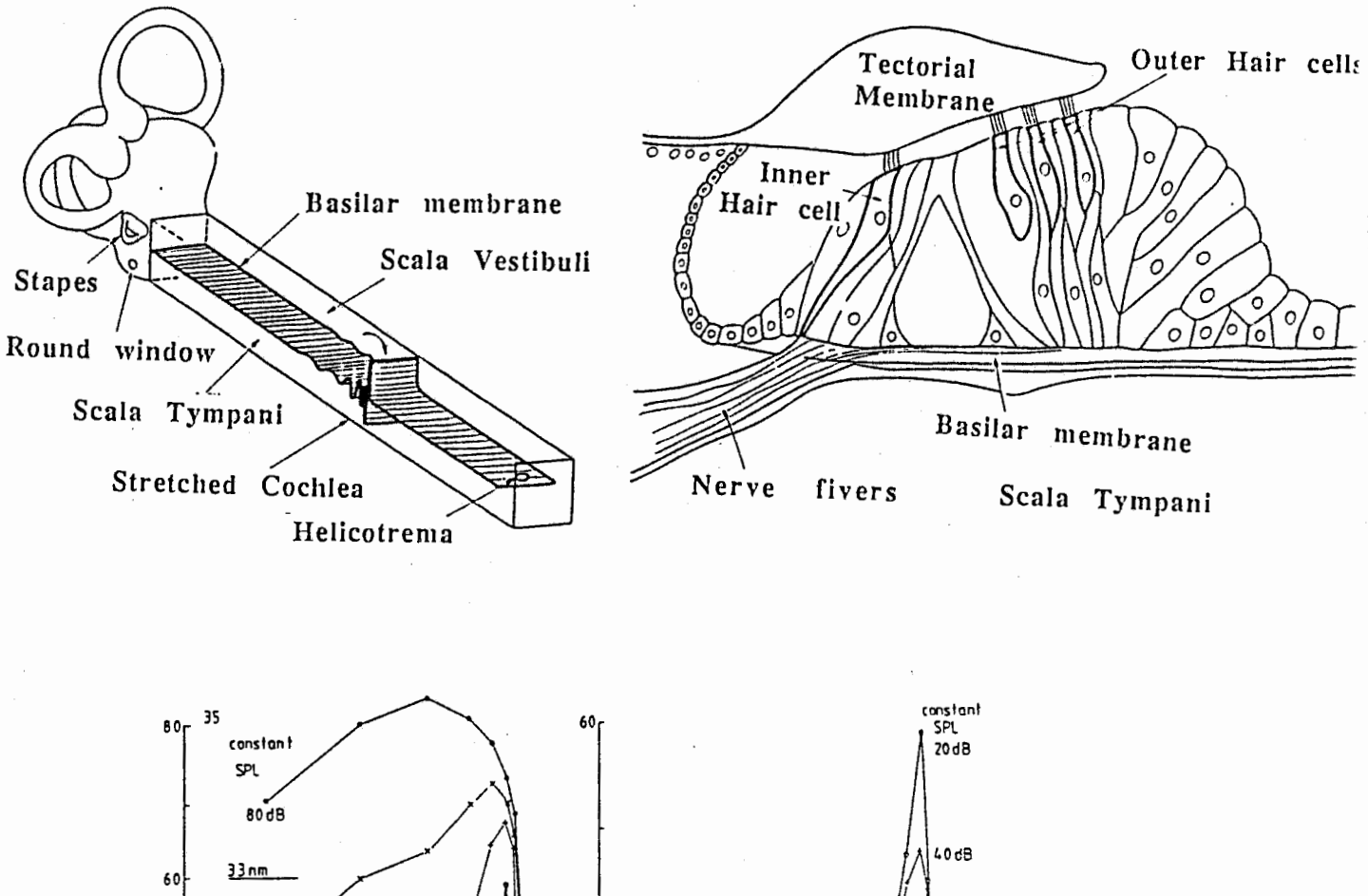

Fig.1 Basilar membrane response envelope at four sound pressure levels (after B.M.Johnstone *et al.*)

Adaptive Q Circuit

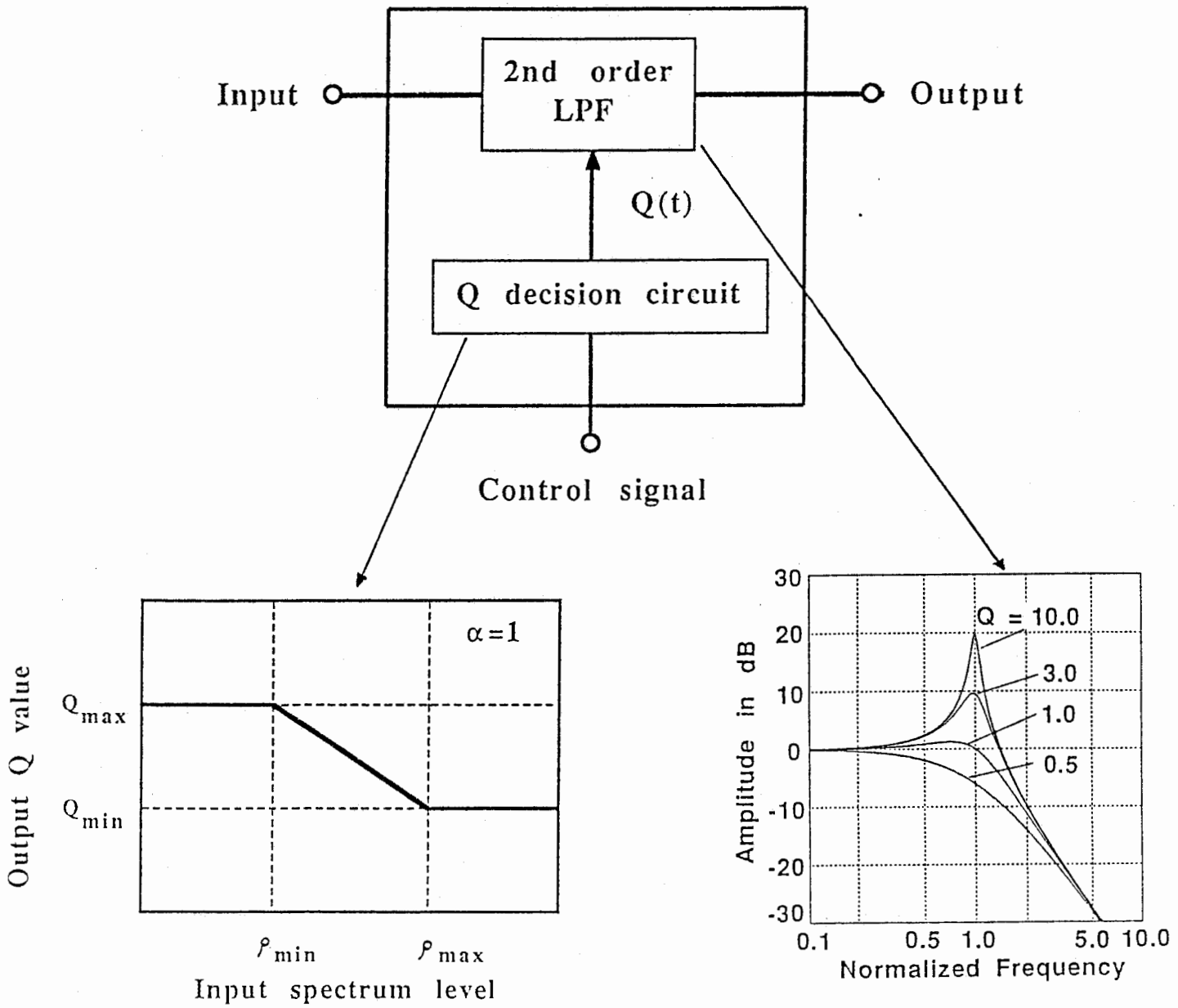

Fig.2 Block diagram of the adaptive Q function (upper), frequency response of a 2nd order Low Pass Filter at four Q values (bottom left) and Input-output relationship of a Q decision circuit, which calculates 2nd order LPF Q from control signal by formulae [5] [6] and [7]. (bottom right)

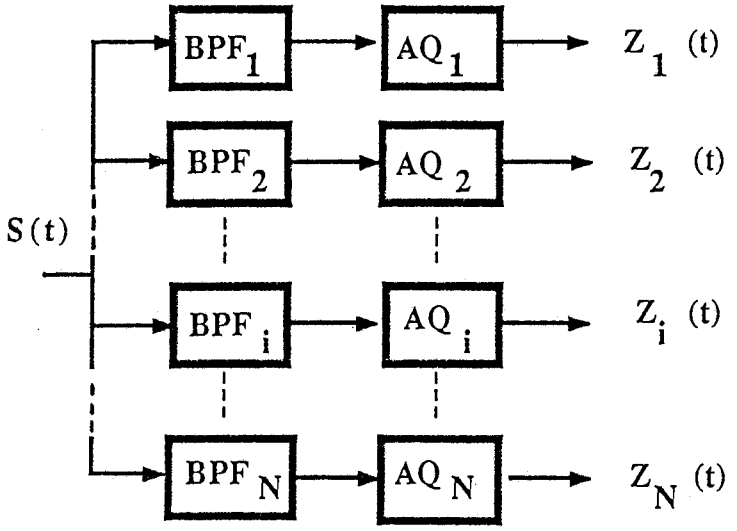

(a) Parallel Adaptive Q Filter-bank

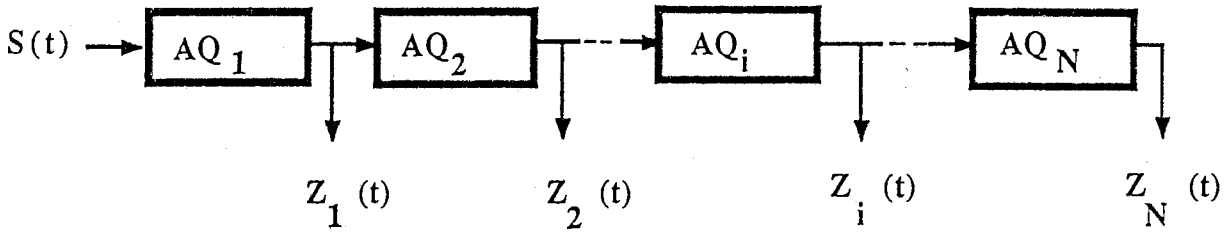

(b) Cascade Adaptive Q Filter-bank

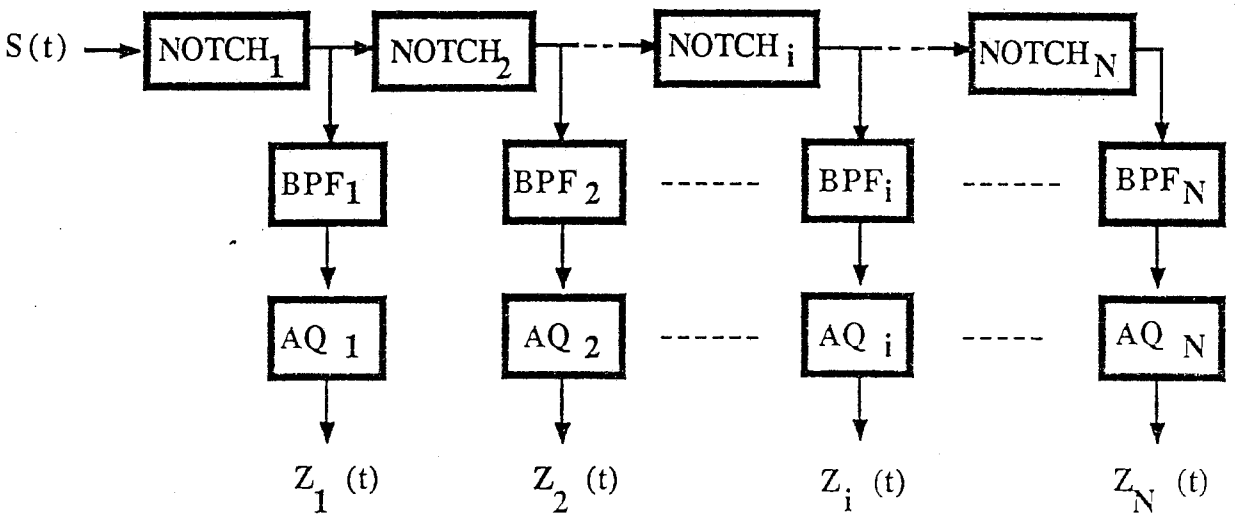

(c) Cascade/parallel Adaptive Q Filter-bank

Fig.3 Block diagram of cascade/parallel type adaptive Q filter-banks.

Block Diagram of the Model

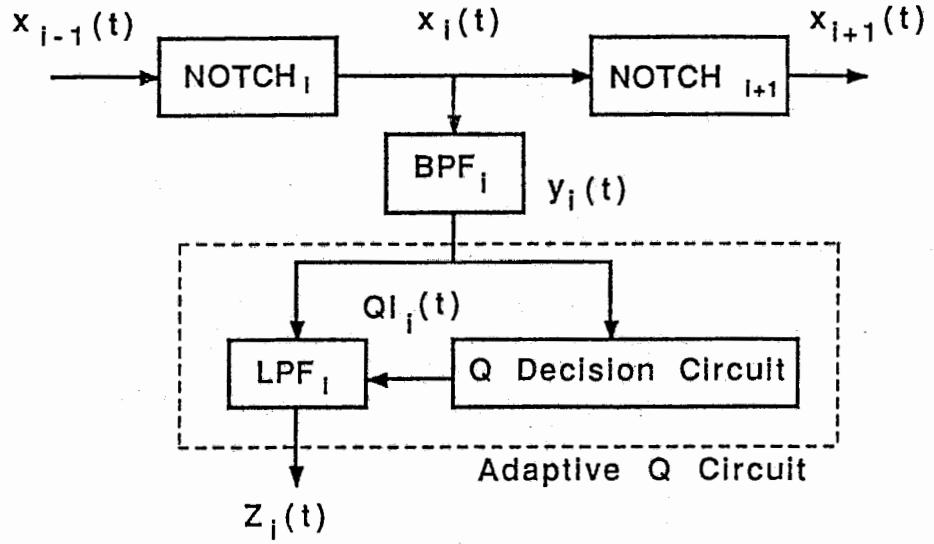

$$NOTCH_i(s) = \frac{\omega p_i^2}{\omega z_i^2} \cdot \frac{s^2 + (\omega z_i / Qz_i)s + \omega z_i^2}{s^2 + (\omega p_i / Qp_i)s + \omega p_i^2}$$

$$BPF_i(s) = \frac{(\omega b_i / Qb_i)s}{s^2 + (\omega b_i / Qb_i)s + \omega b_i^2}$$

$$LPF_i(s) = \frac{\omega l_i^2}{s^2 + (\omega l_i / Ql_i)s + \omega l_i^2}$$

Qp_i : Channel dependent

Qz_i : Channel independent

Qb_i : Channel independent

Ql_i : Channel and time dependent

$Rn = \omega p_i / \omega z_i$ = Constant

$Rb = \log(\omega z_i) / \log(\omega b_i)$ = Constant

$Rl = \omega b_i / \omega l_i$ = Constant

Fig.4 i-th section block diagram of the proposed nonlinear cochlear filter with adaptive Q circuits.

Table 1 Transfer functions and parameters of the model.

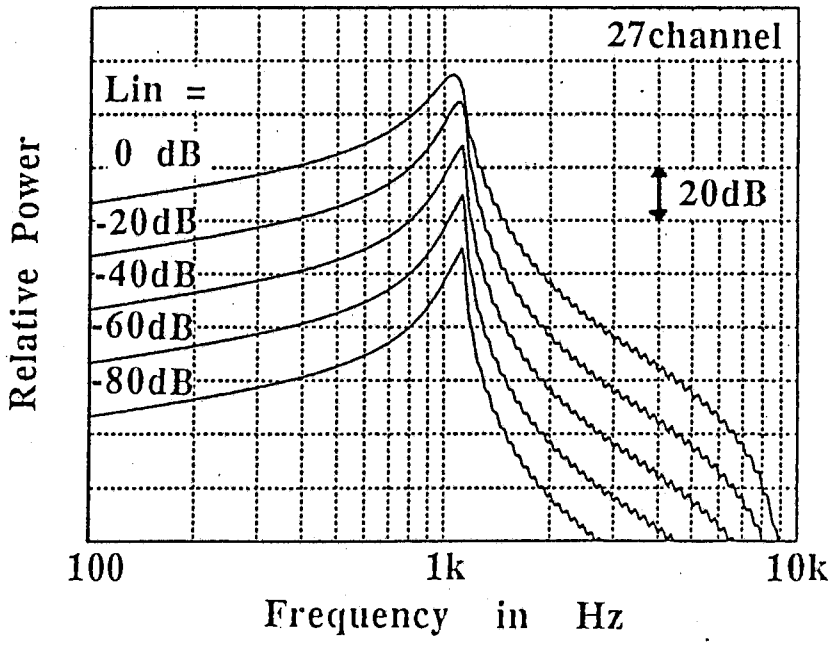

Fig.5 Level response of the 27th channel (9Bark) as a function of frequency.

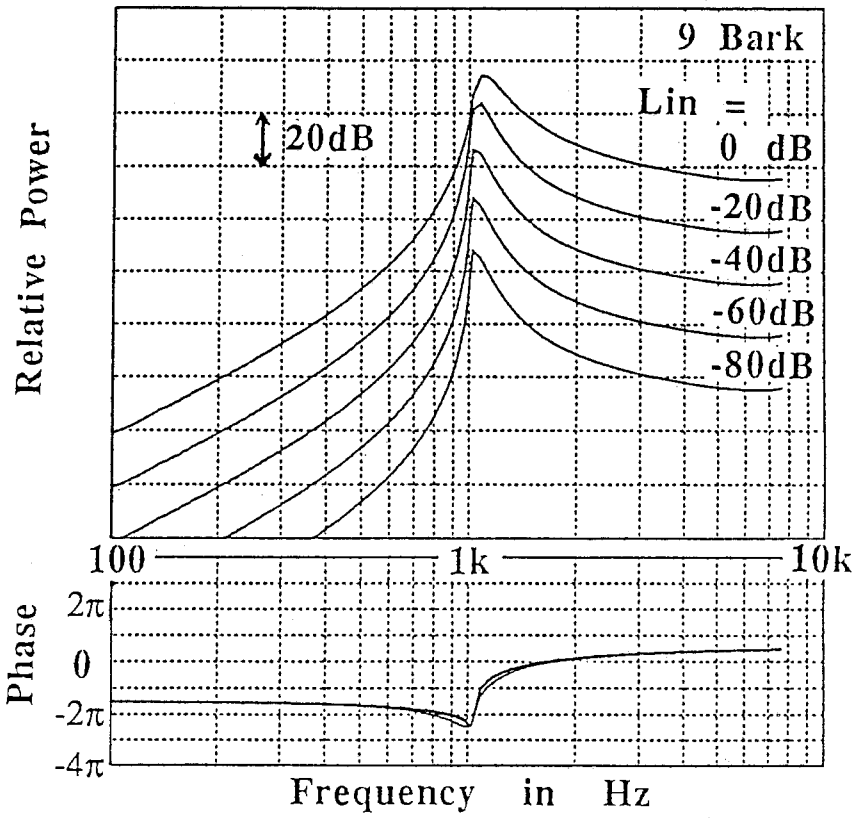

Fig.6 Level and phase response as a function of place with the input signal level. Input signal is 9 bark.

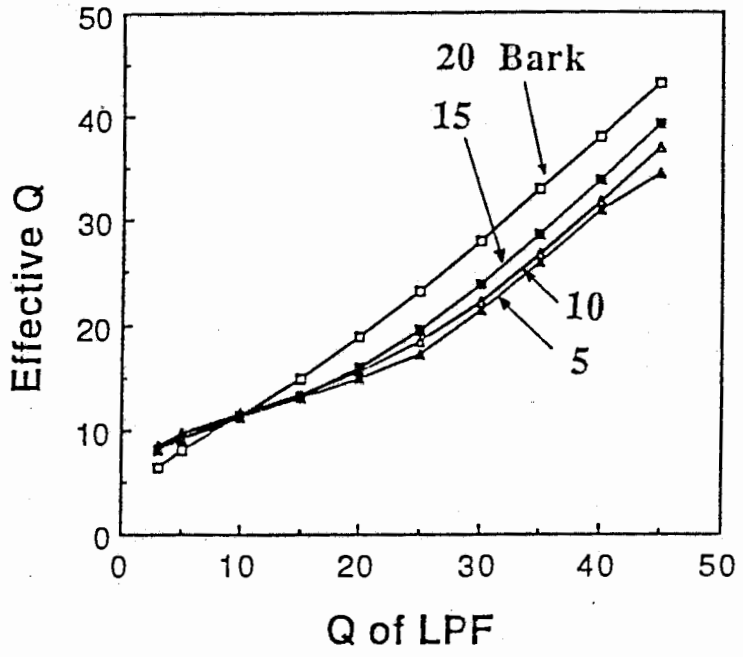

Fig. 7 Effective Q as a function of LPF's Q.

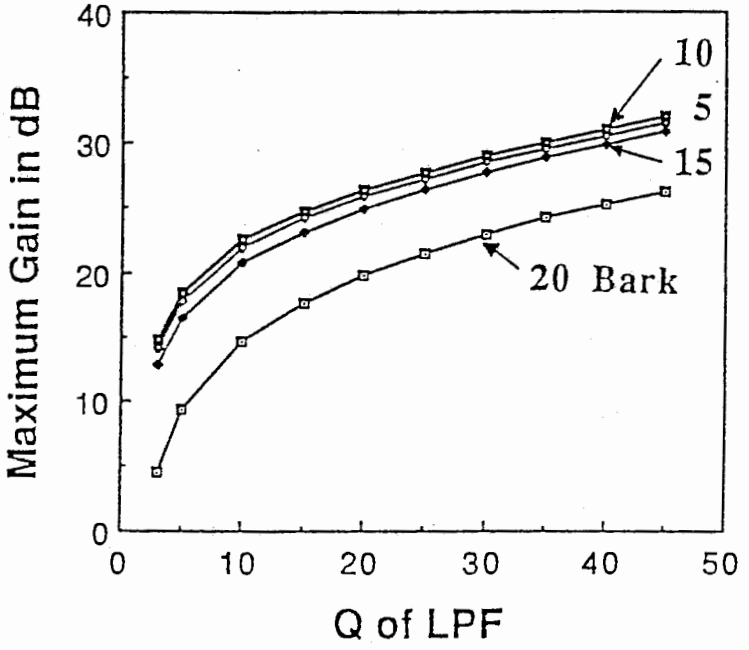

Fig. 8 Maximum gain of several channels as a function of LPF's Q

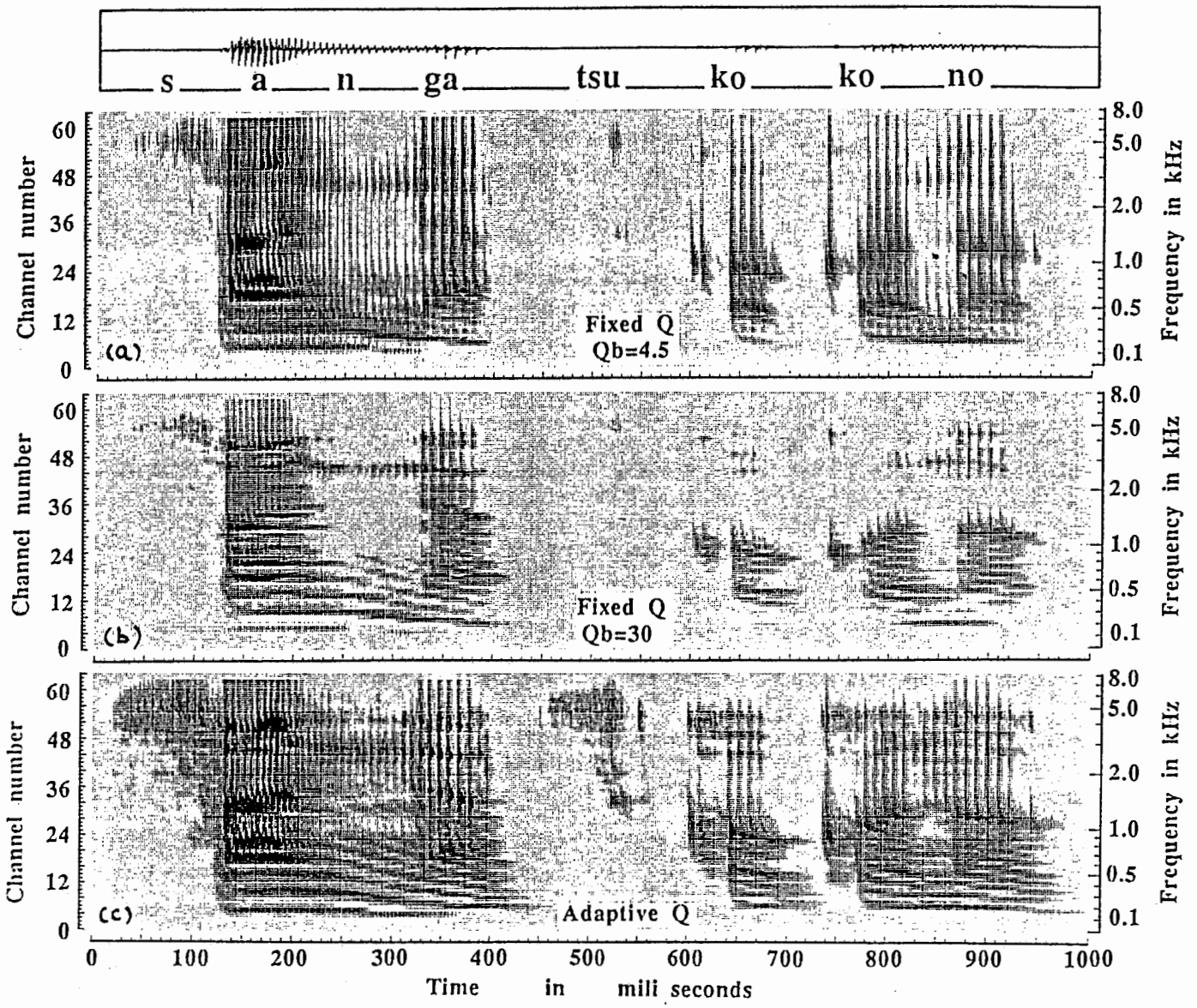

Fig.9 Sound spectrogram obtained by three types of cochlear filter-banks. (a) and (b) are obtained by a cascade/parallel linear cochlear filter bank without adaptive Q circuits: Qb = 4.5 (a) and Qb = 30 (b). (c) is obtained by a cascade/parallel nonlinear cochlear filter bank with adaptive Q circuit. Each filter bank has 61 channels covering 1 to 21 barks spaced by every 1/3 Bark. In the analysis, frame rate and frame length are 2 msec. without overlapping. The averaged logarithmic power level are plotted with 36 gray levels with an 80dB dynamic range.

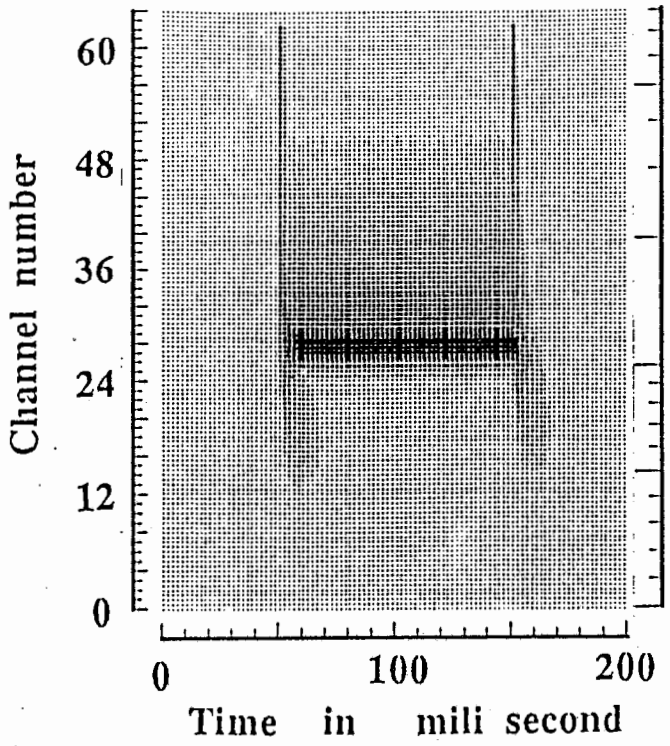

Fig.10 Sound spectrogram of a pure tone burst (9Bark) obtained by the nonlinear cochlear filter with adaptive Q circuits.

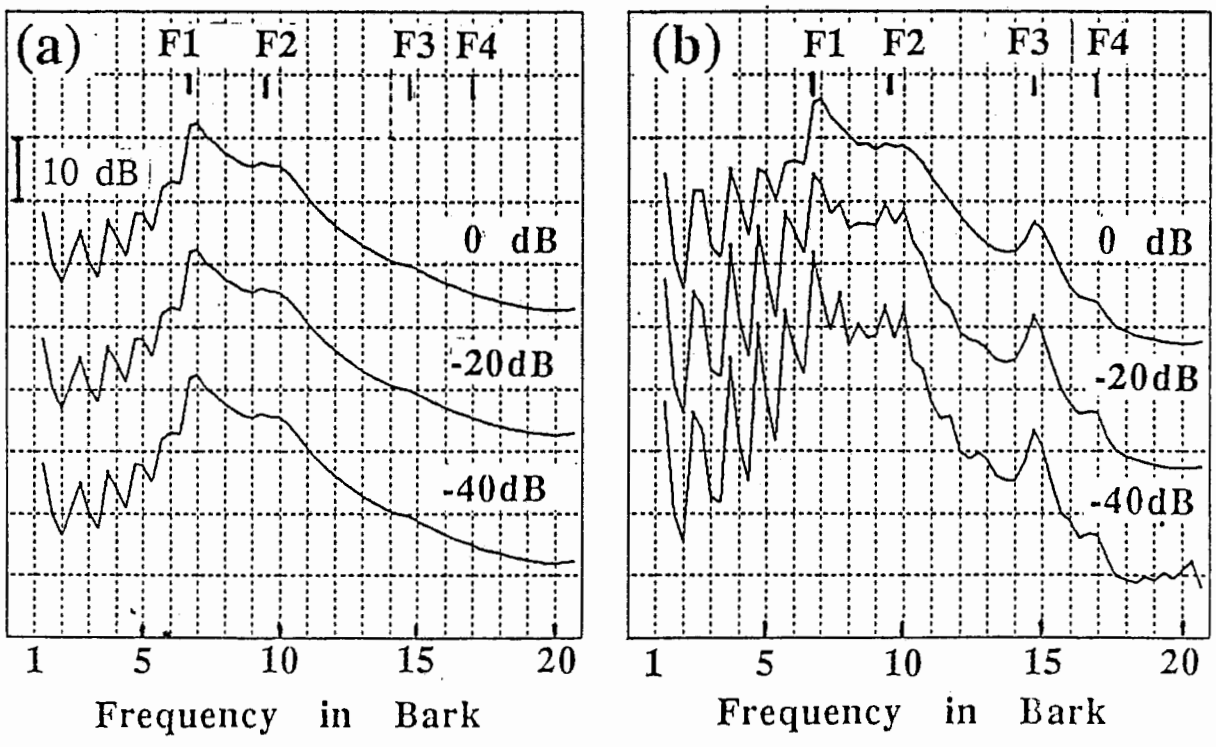

Fig. 11 Spectral slices of synthesized vowel /a/. (a) is obtained by the linear cochlear filter bank with fixed Q (Qb = 4.5) (b) is obtained by the nonlinear cochlear filter bank with adaptive Q circuit. Analysis window is 15 msec. rectangular window.